J. Chem. Thermodynamics 42 (2010) 1435–1440

Contents lists available at ScienceDirect

J. Chem. Thermodynamics

journal homepage: www.elsevier.com/locate/jct

Hybridization thermodynamics of DNA bound to gold nanoparticles

Brian Lang

National Institute of Standards and Technology, Gaithersburg, MD 20899, USA

ARTICLE INFO

Article history:
Received 19 May 2010
Received in revised form 25 June 2010
Accepted 28 June 2010
Available online 8 August 2010

Keywords:
Isothermal Titration Calorimetry
DNA
Nanoparticles

ABSTRACT

Isothermal Titration Calorimetry (ITC) was used to study the thermodynamics of hybridization on DNA-functionalized colloidal gold nanoparticles. When compared to the thermodynamics of hybridization of DNA that is free in solution, the differences in the values of the Gibbs free energy of reaction, $\Delta_r G°$, the enthalpy, $\Delta_r H°$, and entropy, $\Delta_r S°$, were small. The change in $\Delta_r G°$ between the free and bound states was always positive but with statistical significance outside the 95% confidence interval, implying the free DNA is slightly more stable than when in the bound state. Additionally, ITC was also able to reveal information about the binding stoichiometry of the hybridization reactions on the DNA-functionalized gold nanoparticles, and indicates that there is a significant fraction of the DNA on gold nanoparticle surface that is unavailable for DNA hybridization. Furthermore, the fraction of available DNA is dependent on the spacer group on the DNA that is used to span the gold surface from that to the probe DNA.

Published by Elsevier Ltd.

1. Introduction

DNA oligonucleotides bound to substrates are increasingly being used for a multitude of analytical and diagnostic techniques. One of the primary applications is DNA microarray technology – a valuable tool that allows for massively parallel studies of gene expression [1]. Similarly, DNA-functionalized gold nanoparticles are being increasingly utilized in diagnostic tests [2,3]. One of the advantages of these techniques is that the interactions of interest are confined into small and well defined footprints. These applications and their variants rely on the bound DNA hybridizing with its complement (either DNA or RNA) to generate the required signal for data processing. The selectivity of these measurements is based on the higher binding affinity to the complementary nucleic acid strand over competing nucleic acids with one or more mismatched bases. The overall sensitivity and detection limit is related directly to the signal measured from hybridized nucleic acids as a measure of the total number of bound target molecules. Ultimately, it is the thermodynamics (*i.e.* a knowledge of the equilibrium constant, the standard Gibbs free energy, *etc.*) of the probe to target molecule binding reaction that is the essential component in optimizing the signal.

For a first estimate of the thermodynamics of the DNA hybridization reaction on a substrate, methods such as the Nearest Neighbor Model can be used [4,5]. However, models such as these make predictions based on free DNA in solution and do not consider a system with potentially fewer degrees of steric freedom. How the thermodynamics of the binding reaction change as it is moved from a free to a bound condition is an essential component. In some respects, it may be assumed that the free energy of hybridization does not change from the free to the bound state. From the structure of the DNA double helix, the DNA hybridization reaction is dependent only on the hydrogen bond interaction between the pyridine and pyrimidine bases. Therefore, if there are no structural or conformational differences between the two states, the binding enthalpy of the hybridization reaction is not expected to change from the free to the bound state.

However, the potential changes in entropy are expected to influence the thermodynamics. By affixing DNA to a surface, there is an inherent reduction in the total degrees of freedom for the molecular motion that should decrease the entropy change of the hybridization reaction. In addition, there are other interactions in which DNA hybridization may be influenced by tethering the single-stranded DNA to a surface. First, because of the close proximity to a surface and other DNA strands, steric interactions are thought to potentially lower the binding enthalpy and free energy. Second, some molecular modeling predicts that the binding free energy of DNA duplex interactions near the surface tether may actually increase [6]. Ultimately, it is the sum of all of these interactions that affect the measurable and critical thermodynamics of the surface bound DNA hybridization reactions.

The thermodynamics of DNA hybridization bound to gold nanoparticles has been investigated numerous times in the past several years [7–12]. These studies were aimed to serve as a model for any system where DNA is bound to a substrate. But, generally these investigations have been melting type studies that have used either fluorophore quenching or the changes in hydrodynamic radius of the particles to determine the binding thermodynamics. There is little consensus of results between the various methods, in fact

E-mail address: brian.lang@nist.gov

0021-9614/$ - see front matter Published by Elsevier Ltd.
doi:10.1016/j.jct.2010.06.013

discrepancy seen between some of the methods has been so great that there is both positives and negative differences in the free energy of binding between the free DNA hybridization and substrate bound DNA hybridization for the same DNA sequence [8,12]. Furthermore, the literature reports a significant enthalpy difference between the bound and free DNA hybridization reaction, typically greater than 10 kJ · mol^{-1}. Thus, part of the aim of this work is to resolve some of the discrepancies presented in the literature and to understand better the hybridization thermodynamics by using a method independent of some of the bias in the melting studies.

We use Isothermal Titration Calorimetry (ITC) to measure the equilibrium constant, K, and the enthalpy of reaction, $\Delta_r H°$, for the substrate bound DNA hybridization reaction. ITC has the advantage of directly measuring the enthalpy change of the binding reaction as a function of the complementary DNA strand titrated in. The calculation of the free energy from ITC uses a one site binding model assuming a relatively fast binding reaction rate and is concentration independent. This is opposed to melting studies that assume that the DNA melting is a two-state system where there is an equal distribution between double stranded and single-stranded DNA at the observed melting temperature and is a function of concentration. Furthermore, the thermodynamic parameters derived from ITC are measured for a specific temperature (in this case T = 310 K (37 °C) rather than being extrapolated from higher temperatures. All of the thermodynamic data presented for substrate bound DNA from previous studies have been based on melting type measurements [8,11–14], yet there have been no studies found that use ITC or a similar technique. Although ITC requires higher sample concentrations than melting studies, it is a more direct technique for resolving the thermodynamic parameters of DNA hybridization.

2. Experimental

2.1. Materials

The oligonucleotides for this study (see table 1) were purchased from Operon Biotechnologies (Huntsville, AL) [15]. The oligos were then purified by polyacrylamide gel electrophoresis, and desalted using a NAP-5 column from G.E. biosciences. Oligos used in this study are listed in table 1. Oligo **6** is the same as the strand used in the Lytton-Jean and Xu papers, with oligos **5** and **7** being variants with poly-T and c18 linker groups [8,12]. Once desalted, the oligonucleotides were dissolved in deionized water, divided into several aliquots, and then dried using a speed-vac system. Gold colloids (20.2 nm diameter) were purchased from Ted Pella Inc. (Redding, CA) and used as obtained.

2.2. DNA–Au colloid preparation

The solutions of DNA–Au colloid were prepared after the method reported by Hurst *et al.* [16], with modifications which are now described. Briefly, one of the dried aliquots of disulfide modified DNA was dissolved in 0.001 cm^3 of freshly prepared 0.1 m dithiothreitol (DTT), 0.18 m phosphate buffer (pH 7.01) for 1 h at T = 296 K to cleave the disulfide bond.[1] The oligo was separated from the excess DTT and other reaction products using a NAP-5 column. The purified oligonucleotide in 0.18 M phosphate buffer (PB) was added to 25 cm^3 of 20.3 nm gold colloid solution. The PB concentration was then brought up to 10 mm and sodium dodecyl sulfate (SDS) was added up to 0.01 %(m/v). The solution was sonicated for 1 min and then allowed to incubate for 20 min at room temperature. The sodium chloride concentration was increased to 1 m in 0.1 m increments by the addition of 2 m NaCl in 0.01 m PB. This was followed by sonication and incubation at room temperature after each addition of the NaCl/PB solution. The resulting DNA–Au solution was centrifuged at 14,000 RPM to precipitate the Au nanoparticles. The resulting pellet was then re-suspended with 0.01 m PB, 0.01% SDS (we note that subsequent centrifugation generally did not require SDS to re-suspend the Au nanoparticles). Further centrifugation of the DNA–Au particles was performed to rinse the nanoparticles in the working buffer for the ITC experiments, to remove all unbound DNA, and to condense the DNA–Au particles into approximately 2.25 cm^3 of solution.

TABLE 1
Oligonucleotide sequences used in this study. F is the fluorophore 6-FAM. S is a disulfide linkages that is cleaved prior to functionalization to the gold nanoparticle surface.

Oligo	Base sequence (5′ → 3′)
1	S-T_{10}-CGAGACACGGCTAAGTATTGATGCT-F
2	S-A_{10}-CGAGACACGGCTAAGTATTGATGCT-F
3	S-$(CH_2)_{18}$-TCGAGACACGGCTAAGTATTGATGCT-F
4	GCATCAATACTTAGCCGTGTCTCG
5	S-T_{10}-ATCCTTTACAATATT-F
6	S-A_{10}-ATCCTTTACAATATT-F
7	S-$(CH_2)_{18}$-ATCCTTTACAATATT-F
8	AATATTGTAAAGGAT

2.3. Determination of DNA concentration

Concentrations of the free DNA in solution were determined by UV absorption spectroscopy at 260 nm, using a Perkin Elmer Lambda 4B UV/VIS spectrophotometer. The extinction coefficients for the single-stranded DNA and RNA oligomers were calculated based on contributions from the individual bases [17,18]. To determine the concentrations of Au–DNA a digestion technique described by Hurst *et al.* was used [8,19,20]. Briefly, two 0.100 cm^3 aliquots were taken from each solution, an equal volume of 1 m DDT in 0.1 m PB was added to each aliquot and the solutions were allowed to react overnight. In this process the DNA was released from the surface of the gold and the gold nanoparticles became aggregated together. The gold nanoparticles were then removed via centrifugation. A standard curve was made using 6-carboxyfluorescein (6-FAM) labeled DNA of known concentration in PB with a DTT concentration of 0.5 m to keep the pH the same as the test solution; 0.100 cm^3 of the test DNA and standard solutions were loaded onto a 96-well plate. The fluorescence intensity of each well at 520 nm was measured using an excitation source of 495 nm to energize the 6-FAM fluorophore. In all cases, two replicates of the fluorescence measurements were taken. The uncertainty of the concentration of the DNA in the gold nanoparticle colloid is estimated at 5%. This method for determining DNA concentration was validated using Inductively Coupled Plasma-atomic emission spectroscopy (ICP-AES). Two samples of the Au-DNA batches were taken and the phosphate buffer was exchanged for 10 mM sodium cacodylate buffer ($Na(CH_3)_2AsO_2$). The total phosphorus concentration was then measured by ICP-AES, which was then used to calculate the original concentration of DNA in the solutions. Both values were within 4% of the previously measured concentrations. The average DNA loading onto the Au nanoparticles was calculated by dividing the concentration of DNA in solution by the concentration of the nanoparticles as determined by absorption at 530 nm using a molar extinction coefficient of $9.410 \cdot 10^8$ M^{-1} · cm^{-1} (from Ted Pella, Inc.). The surface coverage per square centimeter was determined by dividing the average DNA loading per nanoparticle by the average surface area of the 20 nm nanoparticles (assuming a sphere).

[1] The accepted SI unit of concentration, mol/L, has been represented by the symbol M in order to conform to the conventions of this journal.

2.4. Calorimetry

The DNA hybridization reactions were performed with a Microcal, Inc. VPITC using procedures similar to that of Wiseman *et al.* and Schwarz *et al.* [21,22]. Typically, a nominal 2 μm solution of the Au-DNA would be loaded into the sample cell that was kept thermostated at $T = 310$ K. The injection syringe was filled with a 20 μm solution of the complementary DNA that was titrated into the sample cell as 5 μL aliquots over 30 to 40 injections. The titration run was continued until the addition of the titrant gave a constant energy response, indicating that the reaction had gone to completion. Heats of dilution of the titrant into just the buffer solution were determined and subsequently subtracted from the binding isotherm. The calorimetric titration data were analyzed using Origin software from Microcal Inc., that uses a non-linear least squares minimization method. The resulting fit of the data with a one site binding model gives the equilibrium constant, K, the enthalpy of binding, $\Delta_r H°$, and the stoichiometric ratio of the reaction, N. The entropy change, $\Delta_r S°$, and Gibbs free energy, $\Delta_r G°$, were calculated in the conventional means using K and $\Delta_r H°$. A typical ITC curve and binding isotherm fit where $N = 1$ are shown in figure 1.

Estimated uncertainties in the values of K, $\Delta_r H°$, and N have been calculated for each set of ITC experiments using a Monte Carlo approach. Perturbations of the experimental data sets were generated assuming that there is a 2% uncertainty in the concentration of free DNA, a 5% uncertainty in the concentration of DNA bound to the gold nanoparticles, and a 3% uncertainty in the heats of reaction [23]. One thousand data points were gathered to provide a suitable distribution for the uncertainty. The results of the Monte Carlo analysis give an estimated uncertainty of K between $0.03 \cdot K$ and $0.05 \cdot K$, the uncertainty of $\Delta_r H°$ about $0.03 \cdot \Delta_r H°$, and the uncertainty of N between $0.04 \cdot N$ and $0.05 \cdot N$.

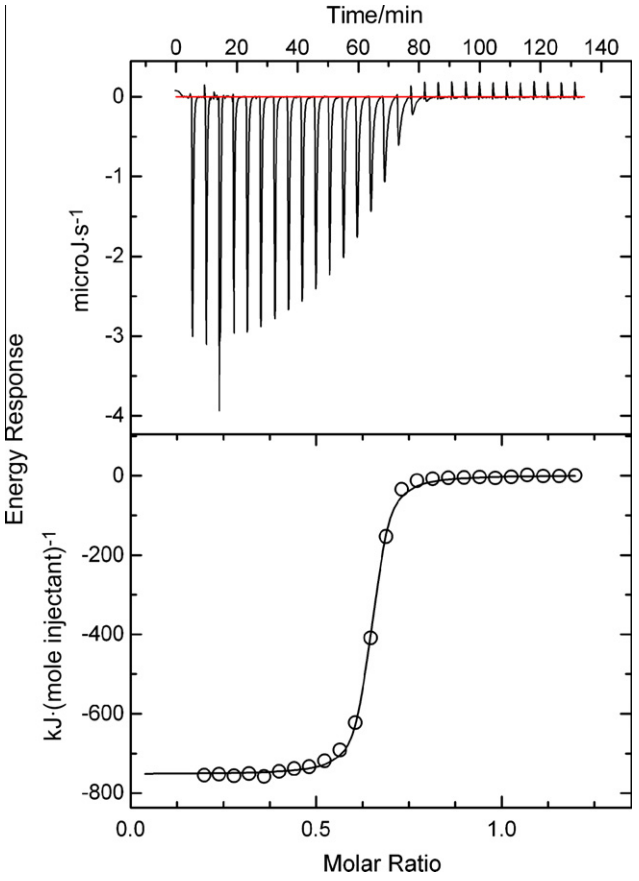

FIGURE 1. Typical ITC data for DNA binding. These data sets are for reaction **Au-1 + 4** displaying (a) the raw ITC scan as the energy response plotted against time reflecting the titration of 5 μL aliquots of oligo **4** into **Au-1** and (b) the integrated titration isotherm with a 1-to-1 binding model fit to the data shown as the energy response per mole of injectant plotted against mole ratio.

3. Results and discussion

Isothermal Titration Calorimetry was initially used to measure the binding constants and enthalpy for the hybridization reaction of oligos **1** and **4** (see table 1), first run with the DNA free in solution (**1 + 4**), then repeated where oligo **1** was bound to the surface of the gold nanoparticles (**Au-1 + 4**). Subsequently, ITC was used to characterize the reactions: **2 + 4** and **Au-2 + 4**; **3 + 4** and **Au-3 + 4**; **5 + 8** and **Au-5 + 8**; **6 + 8** and **Au-6 + 8**; and **7 + 8** and **Au-7 + 8**. All measurements were made under the same conditions with the exception of **3 + 4** and **Au-3 + 4**, where the buffer was adjusted to 0.05 mass% SDS due to issues with keeping the Au nanoparticles in solution. The thermodynamic data from the fits of the integrated ITC experiments are given in table 2. The data presented in the table represent at least two replicate ITC measurements, with exception of reactions **3 + 4** and **Au-3 + 4**, due to the low yield of the oligo **3** received. Uncertainties given in the table are a combination of random uncertainties from the standard deviations of the experimental data, and estimated systematic uncertainties derived from the Monte Carlo simulations. The random and estimated uncertainties were combined and the values presented in table 2 represent the uncertainty at the 95% confidence interval.

From the data presented in the table, there are only small differences in the enthalpy of hybridization between the free and bound states of DNA. A statistical significance test for the enthalpies suggests that there is no difference in $\Delta_r H°$ between the free and bound states for the various reactions at the 95% confidence interval. The difference in $\Delta_r H°$ between the free to bound hybridizations in this study is less than those published in previous studies [8,12], even when the current work uses some oligos that are longer than those in the literature. (A longer oligo will generate a larger total enthalpy, since it is additive, and may potentially yield a larger difference between free and bound states.) Furthermore, applying a t-test to the enthalpies from literature shows that not all of the literature data reveal a significant variance of the enthalpies.

In a similar analysis of the Gibbs free energy of hybridization, the difference in $\Delta_r G°$ between free and bound DNA for reactions of oligos **1**, **2, 5**, and **6** show differences of 3 kJ · mol^{-1}, 1 kJ · mol^{-1}, 2 kJ · mol^{-1}, 3 kJ · mol^{-1}, respectively. Reactions involving oligos **3** and **7** will be discussed below. The significance test for these two pairs of reactions shows that there is a meaningful difference between the values of $\Delta_r G°$ in each pair (being just outside of experimental uncertainty). However there is a general trend for all the data, since Gibbs free energies for all of the bound DNA reactions are all less than the corresponding free reactions, suggesting the possibility of a slight decrease in the overall binding free energy for the bound DNA. When compared with $\Delta_r G°$ differences reported elsewhere, the differences in $\Delta_r G°$ are typically one third of reported values. A direct comparison of the change in $\Delta_r G°$ in this study with that in the literature is difficult since in this current work $\Delta_r G°$ (as derived from K) is calculated directly from the change of q (heat) with respect to the change in mole fraction of the titrant, whereas in the melting studies, $\Delta_r G°$ is calculated from $\Delta_r H°$ and $\Delta_r S°$ extrapolated from higher temperatures [8,12,24,25]. Since the determination of $\Delta_r G°$ in this study is measured quasi-independent of the other thermodynamic parameters, it may be seen as more reliable and will be less influenced by the propagation of error [23]. The change in $\Delta_r G°$ between reactions **3 + 4** and **Au-3 + 4** is notably larger than the other sets of reactions presented here, and is statistically significant. The added SDS is a potential contributor to the difference since the SDS could shield the large charge density from the phosphate groups of the DNA on the gold surface [26,27]. However, we do not suppose that it is due to the presence of SDS in these reactions, since we demonstrate elsewhere that there in no difference in the thermodynamic parameters of free and bound DNA with the addition of SDS (see Supplementary material). Other sources of this difference will be elucidated subsequently.

Also of interest is the overall stoichiometry of the reactions. For the ITC experiments, the stoichiometry of the reaction, N, is derived directly from the fit of the titration curve. Conceptually, it is the mole of titrant per mole of titrand and it is calculated from the value of the mole fraction the titrant at the inflection point of the titration curve. In a system like the DNA hybridization reaction, N should be exactly one, since binding of a single-strand of DNA to its complement is a 1:1 stoichiometric ratio. However, factors such as possible errors in the concentrations and other interactions with the binding sites can cause N to deviate from unity. This is seen in all of the free oligo reactions where N is found to be between 0.92 and 1.05. However, in all cases $N = 1$ within the 95% confidence intervals of uncertainty. Previous experience with the DNA hybridization reactions indicates that this small deviation may be due to possible errors in the concentration of the titration solutions [23,28]. The shift in N for the bound DNA reactions is substantially further away from one than the free DNA in solution, as shown in table 2 and figure 2 illustrates this using the integrated ITC curves and fits for the free and bound hybridization reactions for oligos **5**, **6**, and **7**.

TABLE 2
DNA hybridization thermodynamics in solution and on gold nanoparticles (Au) as determined by the fit to the ITC titration curve. The stoichiometric ratio, *N*, for the reaction based on the fit is given as well. Uncertainties given are the combined random and estimated uncertainties and represent uncertainty at the 95% confidence interval.

Reaction		K'	$\Delta_r H°/(kJ \cdot mol^{-1})$	$\Delta_r G°/(kJ \cdot mol^{-1})$	$\Delta_r S°/(J \cdot K^{-1} \cdot mol^{-1})$	N
			T_{10}			
1 + **4**	(Free)	$(8.6 \pm 3.5) \times 10^8$	−799 ± 26	−53.1 ± 1.8	−2405 ± 84	0.92 ± 0.08
Au-1 + **4**	(Bound)	$(2.6 \pm 2.2) \times 10^8$	−795 ± 31	−50.0 ± 1.5	−2402 ± 100	0.64 ± 0.09
			A_{10}			
2 + **4**	(Free)	$(9.0 \pm 1.8) \times 10^6$	−432 ± 26	−41.3 ± 0.8	−1257 ± 84	0.97 ± 0.05
Au-2 + **4**	(Bound)	$(7.0 \pm 2.5) \times 10^6$	−454 ± 37	−40.2 ± 1.4	−1332 ± 110	0.21 ± 0.05
			c18			
3 + **4**	(Free)	$(5.1 \pm 1.0) \times 10^8$	−649 ± 21	−52.0 ± 0.9	−1925 ± 68	0.92 ± 0.08
Au-3 + **4**	(Bound)	$(3.4 \pm 0.8) \times 10^8$	−659 ± 27	−44.7 ± 0.8	−1980 ± 84	0.44 ± 0.07
			T_{10}			
5 + **8**	(Free)	$(6.9 \pm 1.0) \times 10^6$	−398 ± 16	−40.6 ± 0.8	−1155 ± 52	0.94 ± 0.10
Au-5 + **8**	(Bound)	$(3.8 \pm 0.9) \times 10^6$	−404 ± 18	−38.8 ± 1.1	−1178 ± 58	0.48 ± 0.06
			A_{10}			
6 + **8**	(Free)	$(8.4 \pm 2.2) \times 10^6$	−440 ± 22	−41.1 ± 1.5	−1285 ± 70	1.05 ± 0.10
Au-6 + **8**	(Bound)	$(2.6 \pm 0.6) \times 10^6$	−473 ± 29	−38.1 ± 1.0	−1403 ± 95	0.33 ± 0.10
			c18			
7 + **8**	(Free)	$(6.6 \pm 2.0) \times 10^6$	−397 ± 12	−40.5 ± 1.0	−1150 ± 38	0.93 ± 0.09
Au-7 + **8**	(Bound)	$(8.2 \pm 2.5) \times 10^5$	−392 ± 102	−35.1 ± 0.9	−1151 ± 330	0.14 ± 0.10

Because the values of *N* for the bound DNA are so far from one, it was deemed necessary to examine possible sources of error to validate our results. An obvious and most likely source of error is any inaccuracy in the concentration of the DNA on the gold nanoparticles that would in turn effect the calculation of *n* when evaluating the titration curves. We believe that the concentration of oligos **4** and **8** (the titrants) is accurate, since its concentration was determined directly by UV absorption. Thus, most of the error is judged to lie with the concentration of the DNA on the gold nanoparticles. To examine the effect of any inaccuracy of the Au–DNA solutions, we simulated the effect of different Au–DNA concentrations by reanalyzing the titration curves with the fitting program by adjusting the concentration of the cell solution in Origin until *N* became equal to 1. To get the desired value of $N = 1$, the value of the Au–DNA colloid concentration had to be substantially decreased in the fitting program. This is in contrast to the assumption that the DNA concentrations resulting from the digestion method would be a lower limit to the concentration, since it might not be possible to recover all the DNA from the gold nanoparticles. Also, the change in the adjusted concentration used for fitting was well outside of the concentration range determined using ICP-AES. Furthermore, when the adjusted concentrations were used in fitting the titration curves, the resulting values of K, $\Delta_r G°$, $\Delta_r H°$, and $\Delta_r S°$ were within the uncertainty of the original values. For instance, with reaction **Au-1** + **4** when the concentration was changed from 2.32 μM to 1.51 μM, the stoichiometry changed from $N = 0.64$ to $N = 1.01$, while the binding constant only changed from $K = 2.6 \cdot 10^8$ to $K = 3.1 \cdot 10^8$, and the heat of reaction changed from $\Delta_r H° = -795\ kJ \cdot mol^{-1}$ to $\Delta_r H° = -779\ kJ \cdot mol^{-1}$. This gives changes of $0.5 \cdot 10^8$ and $-16\ kJ \cdot mol^{-1}$ for K and $\Delta_r H°$, respectively, which is less than the corresponding 95% confidence intervals of $\pm 2.2 \cdot 10^8$ and $\pm 31\ kJ \cdot mol^{-1}$ (refer to table 2). Therefore, we conclude that the concentrations of the Au–DNA used in the original titration curve fitting are reasonably accurate and are likely not the source of the deviance of *N* from one.

Based on the above, we conclude that values of *N* for the bound DNA hybridizations are representative of the actual stoichiometry of the reaction. This implies that a significant fraction of the DNA on the nanoparticle surface is inaccessible for hybridization. The binding stoichiometries for reactions **Au-1** + **4**, **Au-2** + **4**, and **Au-3** + **4** are $N = 0.64 \pm 0.09$, $N = 0.21 \pm 0.05$, and $N = 0.44 \pm 0.07$. Likewise the stoichiometries for reactions **Au-5** + **8**, **Au-6** + **8**, and **Au-7** + **8** are $N = 0.48 \pm 0.06$, $N = 0.33 \pm 0.10$, and $N = 0.14 \pm 0.10$, respectively. We attribute this to varying environments of the DNA on the gold surfaces that reduce binding. Possible causes of this binding interference are steric interference from neighboring DNA strands, the highly localized negative charges of the DNA clustering in one area, or interactions of the bound DNA with the gold surface that block hybridization [1,6,13,29,30]. One environmental factor that can contribute to the binding accessibility is the surface density of the DNA on the gold nanoparticles. This is easily calculated since the concentrations of the DNA and the size of the nanoparticles are known and the number of gold nanoparticles in suspension is readily established from the absorbance at 530 nm (see section 2.3). We determined that for the solutions of **Au-1**, **Au-2**, and **Au-3** there are (186 ± 45), (181 ± 10), and (86 ± 30) strands of DNA per nanoparticle with a surface coverage of $(1.44 \pm 0.24)10^{13}$, $(1.40 \pm 0.05)10^{13}$, and $(6.90 \pm 0.54)10^{12}$ strands per cm^2, respectively. For **Au-5**, **Au-6**, and **Au-7** there are (200 ± 50), (323 ± 30), and (338 ± 58) strands of DNA per nanoparticle with a surface coverage of $(1.59 \pm 0.37)10^{13}$, $(2.50 \pm 0.25)10^{13}$, and $(2.61 \pm .45)10^{12}$ strands per cm^2, respectively. The coverage of the DNA on the gold surfaces is within what has been reported and also matches the density reported for some DNA microarrays [13,14,19,29]. There is some variability between the different preparations of Au–DNA for a given oligo (part of this is seen in the uncertainties) and all of the preparations except that of **Au-3** are within 25% of the median value. Using the calculated surface coverage, we find that there is no correlation between DNA surface coverage and the binding reaction stoichiometry. Oligos **1** and **2** have a similar average surface coverage on the nanoparticles, yet there is a three fold difference in calculated *N*. Similarly, oligos **6** and **7** have about the same surface coverage, but the difference between values of *N* is even greater. Furthermore, changes in the DNA surface density between the individual samples do not correlate to the changes in the value of *N*.

We propose that the linking group play an important role in the availability of the bound DNA to hybridization. The crucial factor to this may be the spatial configuration of the DNA on the surface of the gold nanoparticles. The conventional view of single-stranded DNA on a surface evokes an image of all the DNA strands sticking straight up (at a normal to the surface) much like a bottle brush. But, in reality, the DNA tends to be in a more random configuration with portions of the strands lying back down onto the surface [20]. It has been shown that strands of poly-A DNA tends to lay down on the a gold surface much more than a poly-T strands [2,8,10]. This would account for the difference in *N* between reactions **Au-1** + **4** and **Au-2** + **4**, and between reactions **Au-5** + **8** and **Au-6** + **8**. In both cases, the strands with the poly-A linking groups have a lower binding stoichiometry than the oligos with poly-T linking groups. The A_{10} linker on oligos **2** and **6** will have a strong tendency to lay down on the gold surface, influencing the probe DNA strand to remain close to the surface, causing many of the DNA strands to be inaccessible to binding.

The effect of the $-(CH_2)_{18}-$ linker is much more difficult to ascertain because the results are not as consistent as with the other two linker types. First, the relative stoichiometries are very different since $N = 0.44$ for the **Au-3** + **4** reaction is between the *N* values of the poly-T and poly-A linkers, while $N = 0.14$ for the **Au-7** + **8** reaction is significantly less than *N* for the other two linkers. Second, the difference in Gibbs free energy between the free and bound states is much more significant than with the other two linkers. For the **Au-7** + **8** reaction, the value of *N* is so low and the curve is so incomplete, that the value of $\Delta_r G°$ derived from the fit may be biased lower because there are not enough data for the model to be fit accurately to the data (refer to figure 2). As for the **Au-3** + **4** reaction, it has a lower surface density of DNA (much less than the other oligos) and may also explain the dramatic change in $\Delta_r G°$ between the free and bound states, since a lower surface density may increase the likelihood of nonspecific binding of DNA to the gold surface. Evidence for nonspecific binding is manifest in the fact that the **Au-3** + **4** gold nanoparticles (post-hybridization reaction) are less prone to aggregation than **Au-3** alone, suggesting that some of the free oligo 4 bound directly to the surface during the titration, and thereby stabilizing the surface and preventing agglomeration. The nonspecific binding would also tend to shift the value of *N* up from where it actually would be, since there are more binding events than just simple DNA hybridization. Thus it is likely that for the **Au-3** + **4** reaction, *N* would be comparable to *N* for the **Au-7** + **8** reaction when all other factors are equal. We note that $-(CH_2)_{18}-$ group is only half as long as the polynucleic acid chains (based on estimates of the molecular structures). This reduced distance from the surface may serve to induce more DNA strands into configurations where they are unable to hybridize.

The differences in stoichiometries, *N*, between the bound and free DNA hybridization reactions may partially explain the differences in thermodynamic parameters based on melting reported in the literature. Typically, melting studies will calculate $\Delta_r S°$ and $\Delta_r H°$ from the relationship of the melting temperature to the

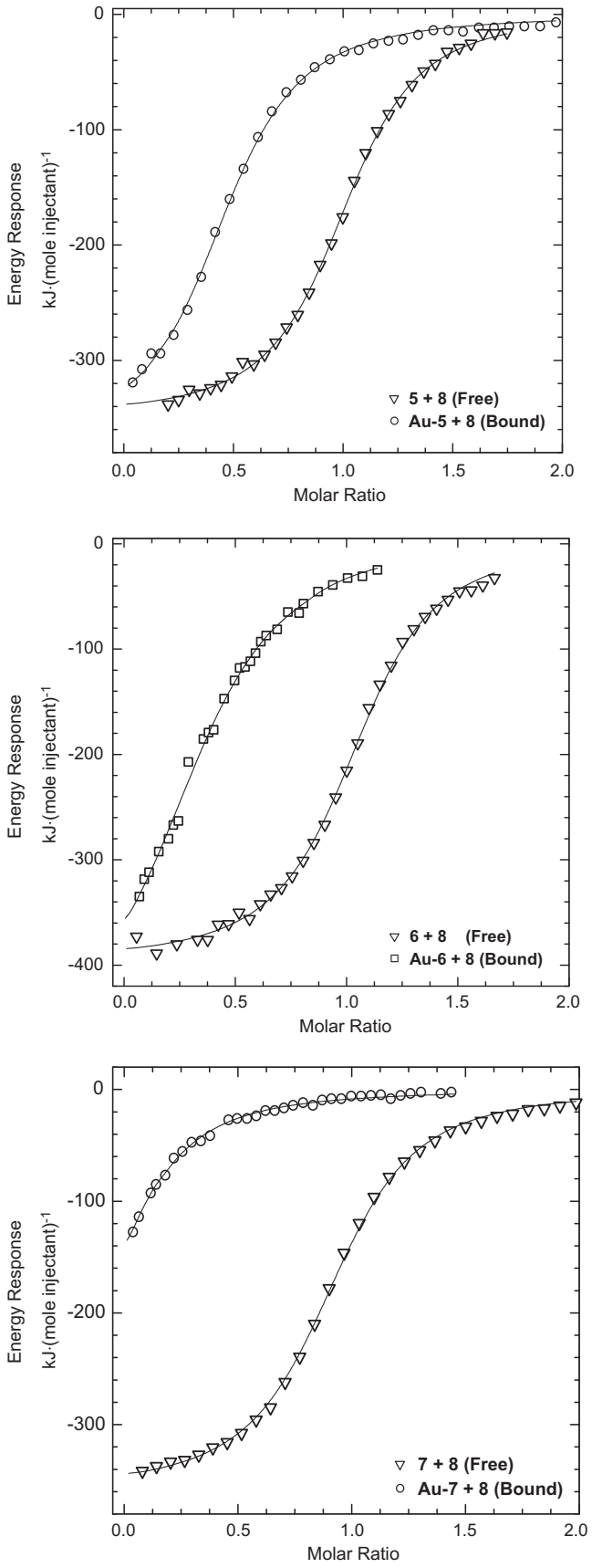

FIGURE 2. Energy response per mole of injectant plotted against mole ratio to show the integrated titration isotherms for the free and bound reactions of (a) the T_{10} linker **5** + **8** (free, ▽) and **Au-5** + **8** (bound, ○); (b) the A_{10} linker **6** + **8** (free, ▽) and **Au-6** + **8** (bound, □), and (c) the $-(CH_2)_{18}-$ linker **7** + **8** (free, ▽) and **Au-7** + **8** (bound, ○)

DNA concentration by using what is essentially the van't Hoff equation [4,8,12]. If the number of DNA molecules on the surface available for binding is significantly less than the total number of DNA molecules bound, the effective concentration of surface DNA will be misrepresented and will skew the calculated thermodynamics. For example, if we estimate that if only 50% of the surface DNA is hybridized, $N = 0.5$, then by calculating K based on this information alone, the result will be orders of magnitude less than an equivalent amount of DNA free in solution. This results in a bias on the calculated K if one is working on the assumption that all the DNA on a surface is available for binding, where we have shown that a significant fraction of the bound DNA in this study does not participate in the binding reactions since K (and $\Delta_r G°$, *etc.*) is essentially unaffected by the different stoichiometric ratios.

Finally, we note that these experiments do not take into account any kinetic factors, such as a slow kinetic rearrangement of the surface tethered DNA that may allow more interactions over a long time period (>24 h). While this may increase the overall N of the reaction in the long term, it still does not affect the thermodynamics, and for practical purposes such as quantitative assays or microarrays, one still wants to optimize the reaction for time and overall sensitivity. However, our own kinetic study indicated that amount of the bound DNA did not increase over time.

4. Conclusions

We have shown that there is little thermodynamic difference between the free and bound DNA hybridization reactions. More importantly, our data suggest that the linker group limits the DNA strands available for hybridization on the bound surfaces. The evidence presented here suggests that a poly-T DNA linking group allows a higher proportion of binding than a poly-A DNA group of the same length. The relative effects of a c18 linker are somewhat more ambiguous, but it appears that it is not as effective as ether the poly-T or poly-A linker. Although we have not addressed all potential linkers of DNA to a substrate, our conclusions is that careful selection of the linker can potentially increase the sensitivity of methods that use bound DNA by maximizing the prospective binding sites.

Acknowledgements

Thanks to Dr. Fred Schwarz (NIST alumnus) for his valuable input on this project, to Dr. Savelas Rabb for work on the ICP-AEWS, and to Dr. David Dewar for his advice on designing the Monte Carlo simulations.

Appendix A. Supplementary data

Supplementary data associated with this article can be found, in the online version, at doi:10.1016/j.jct.2010.06.013.

References

[1] D. Skvortsov, D. Abdueva, C. Curtis, B. Schaub, S. Tavare, Nucl. Acids Res. 35 (2007) 4154–4163.
[2] H. Kimura-Suda, D.Y. Petrovykh, M.J. Tarlov, L.J. Whitman, J. Am. Chem. Soc. 125 (2003) 9014–9015.
[3] J.J. Storhoff, R. Elghanian, R.C. Mucic, C.A. Mirkin, R.L. Letsinger, J. Am. Chem. Soc. 120 (1998) 1959–1964.
[4] J. SantaLucia Jr., Proc. Natl. Acad. Sci. USA 95 (1998) 1460–1465.
[5] J. SantaLucia Jr., H.T. Allawi, P.A. Seneviratne, Biochemistry 35 (1996) 3555–3562.
[6] K.-Y. Wong, B.M. Pettitt, Theor. Chem. Acc. 106 (2001) 233–235.
[7] H. Haick, J. Phys. D 40 (2007) 7173–7186.
[8] A.K.R. Lytton-Jean, C.A. Mirkin, J. Am. Chem. Soc. 127 (2005) 12754–12755.
[9] K.A. Stevenson, G. Muralidharan, L. Maya, J.C. Wells, J. Barhen, T. Thundat, J. Nanosci. Nanotechnol. 2 (2002) 397–404.
[10] J.J. Storhoff, R. Elghanian, C.A. Mirkin, R.L. Letsinger, Langmuir 18 (2002) 6666–6670.
[11] C.S. Thaxton, D.G. Georganopoulou, C.A. Mirkin, Clin. Chim. Acta 363 (2006) 120–126.
[12] J. Xu, S.L. Craig, J. Am. Chem. Soc. 127 (2005) 13231–13277.
[13] A. Halperin, A. Buhot, E.B. Zhulina, Langmuir 22 (2006) 11290–11304.
[14] R. Levicky, A. Horgan, Trends Biotechnol. 23 (2005) 143–149.
[15] The mention or use of products in this manuscript is not meant as an endorsement by NIST nor as an indication that they are the best available.
[16] S. Hurst, A.K.R. Lytton-Jean, C.A. Mirkin, Anal. Chem. 78 (2006) 8313–8318.
[17] M.J. Cavaluzzi, P.N. Borer, Nucl. Acids Res 32 (2004) e13.

[18] J.T. Henderson, A.S. Benight, S. Hanlon, Anal. Biochem. 201 (1992) 17–29.
[19] S.J. Hurst, A.K.R. Lytton-Jean, C.A. Mirkin, Anal. Chem. 78 (2006) 8313–8318.
[20] L.F.I. Pease, D.-H. Tsai, R.A. Zangmeister, M.R. Zachariah, M.J. Tarlov, J. Phys. C: Chem. Lett. 111 (2007) 17155–17157.
[21] F.P. Schwarz, K. Puri, R.G. Bhat, A. Surolia, J. Biol. Chem. 268 (1993) 7668–7677.
[22] T. Wiseman, S. Williston, J.F. Brandts, L.-N. Lin, Anal. Biochem. 179 (1989) 131–137.
[23] F.P. Schwarz, S. Robinson, J.M. Butler, Nucl. Acids Res. 27 (1999) 4792–4800.
[24] K.J. Breslauer, R. Frank, H. Blöcker, L.A. Marky, Proc. Natl. Acad. Sci. USA 83 (1986) 3746–3750.
[25] N. Sugimoto, S.-I. Nakano, K. Misa, A. Matsumura, H. Nakamuta, T. Ohmichi, M. Yoneyama, M. Sasaki, Biochemistry 34 (1995) 11211–11216.
[26] R. D'Agata, R. Corradini, Grasso, Giuseppe, R. Marchelli, G. Spoto, Chem. Biol. Chem. 9 (2008) 2067–2070.
[27] J. Liu, L. Tiefenauer, S. Tian, P.E. Nielsen, W. Knoll, Anal. Chem. 78 (2006) 470–476.
[28] B.E. Lang, F.P. Schwarz, Biophys. Chem. 131 (2007) 96–104.
[29] A. Vainrub, B.M. Pettitt, Phys. Rev. E 66 (2002) 041905.
[30] A. Vainrub, B.M. Pettitt, Biopolymers 68 (2003) 265–270.

JCT 10-171